Geologica Acta, Vol.3, Nº1, 2005, 15-26
Available online at www.geologica-acta.com

geologica acta

Dissolution of minor sulphides present in a pyritic sludge at pH 3 and 25º C

J. CAMA and P. ACERO

Institute of Earth Sciences "Jaume Almera", CSIC
c/Lluís Solé i Sabarís s/n, 08028 Barcelona, Catalonia. Cama E-mail: jcama@ija.csic.es Acero E-mail: pacero@ija.csic.es

ABSTRACT

The steady-state dissolution rates of galena, sphalerite and chalcopyrite at pH 3 under oxygen saturated atmosphere and at 25ºC are obtained by means of non-stirred flow-through experiments. These dissolution rates are compared with those estimated by dissolving pyritic sludge from the Aznalcóllar mining tailings composed of pyrite and minor sulphides galena, sphalerite and chalcopyrite. Based on the respective release of Fe, Pb, Zn and Cu, the steady-state dissolution rates of pyrite ($Rate_{Fe}$), galena ($Rate_{Pb}$), sphalerite ($Rate_{Zn}$) and chalcopyrite ($Rate_{Cu}$) are 6.33 $\pm$ 0.95 x 10^{-11}, 1.2 $\pm$ 0.18x10^{-10}, 1.3 $\pm$ 0.20x10^{-11} and 1.71 $\pm$ 0.25x10^{-11} mol m^{-2} s^{-1}, respectively, yielding $Rate_{Pb} > Rate_{Fe} > Rate_{Zn} \geq Rate_{Cu}$. Based on the release of metal and sulphur to solution, the stoichiometric ratios Pb/S, Zn/S and Cu/S are 4 $\pm$ 0.25, 1.2 $\pm$ 0.1 and 0.90 $\pm$ 0.05 for the respective dissolution reactions of galena, sphalerite and chalcopyrite, which are higher than the ideal ones. These high values result from a sulphur deficit in the output solutions attributed to the loss of H_2S(aq) via gasification by which H_2S(aq) partially converts to H_2S(g). Nevertheless, the Cu/Fe ratio is 0.95 $\pm$ 0.05 during chalcopyrite dissolution at steady state, suggesting that chalcopyrite dissolves stoichiometrically.

KEYWORDS | **Pyritic sludge. Galena. Sphalerite. Chalcopyrite. Dissolution kinetics.**

INTRODUCTION

The sludge produced by the mine at Aznalcóllar (SW Spain) is made up of a mixture of different sulphides. Pyrite is predominant (73 wt. %) and galena, sphalerite and chalcopyrite are only the 0.8, 1.4 and 0.6 wt. %, respectively (Domènech et al., 2002a). The collapse of the tailing dam of the Aznalcóllar pyrite mine (April, 1998) flooded the valleys of the Agrio and Guadiamar rivers with approximately 4 x 10^6 m^3 of sulphidic sludge. After the mechanical removal of the bulk sludge, 0.1 to 5 wt. % of the sludge remained in the unsaturated zone, constituting a pollution risk. The adverse impact on the environment that this remaining percentage of sludge could have for the contaminated area prompted a number of studies on different aspects of the sludge and soil remediation (Ayora et al., 2001a, b; Alastuey et al., 1999; Domènech et al., 2002a, b).

In particular, Domènech et al. (2002a) studied the dissolution kinetics of the pyritic sludge at acidic pH and presented a dissolution rate law of the sludge and pyrite. These authors showed that pyrite dissolution is strongly dependent on the dissolved oxygen concentration and slightly dependent on the environmental acidity. Moreover, based on the release of Pb, Zn and Cu from the

pyritic sludge dissolution, they estimated the dissolution rates of the minor sulphides (galena, chalcopyrite and sphalerite), which did not show any dependence on oxygen concentration or on pH. These results indicate that the processes intervening in the pyrite dissolution can differ from those governing the dissolution of the other sulphides. In contrast to the well-studied mechanism of pyrite dissolution (Lowson, 1982; Mckibben and Barnes, 1986; Nicholson et al., 1988; Moses and Herman, 1991; Rimstidt et al., 1994; Williamson and Rimstidt, 1994; Bonissel-Gissinger et al., 1998; Nordstrom and Alpers, 1999; Rosso et al., 1999; Kamei and Ohmoto, 2000; Domènech et al., 2002a), the dissolution of these minor sulphides has not been fully investigated to date.

Some studies have recently addressed diverse aspects regarding the dissolution of galena, sphalerite and chalcopyrite, utilizing different experimental methodologies. Hsieh and Huang (1989), Fornasiero et al. (1994) and Zhang et al. (2004) investigated the pH effect on the dissolution of galena using batch experiments. The first authors showed that the amount of dissolved Pb(II) decreases with increasing pH from 2.5 to 9 enhanced by dissolved oxygen. Fornasiero et al. (1994) proposed a mechanism of oxidation based on X-ray photoelectron spectroscopy (XPS) and, the last authors proposed a galena dissolution rate law expressed as $r=k[H^+]$ at pH 0.43-2.45 and 25-70ºC.

As for surface processes, Higgins and Hammers (1996) used Electrochemical Scanning Tunneling Microscopy (ECSTM) to investigate the dissolution of galena (001) surfaces immersed in acidic and neutral sulfate electrolyte solutions. These authors suggest that the surface dissolution kinetics under acidic conditions are most likely controlled by desorption of sulfide species from step edges. De Giudici and Zuddas (2001) conducted in situ AFM experiments to characterize the evolution of the galena surface under acidic pH and argued that dissolution of protrusion composed of native sulphur limited the overall dissolution rate.

The effect that iron content in solution could have on the dissolution rates of these sulphides has been studied. Pashkov et al. (2002) observed that galena dissolution was accelerated in the presence of ferric nitrate, showing that a 0.01 M $Fe(NO_3)_3$ solution increased the recovery of lead by a factor of 9. Bobeck and Su (1985) studied the dissolution kinetics of sphalerite in acidic ferric chloride solution at low temperature and obtained an activation energy value of 46.9 KJ mol^{-1} for dissolution.

Leach experiments have also been conducted to study the dissolution of sphalerite and chalcopyrite. Weisener et al. (2003) studied the surface speciation and leaching kinetics of sphalerite particles at pH 1 and temperatures that ranged from 25 to 85ºC. These authors attributed the decrease in Zn dissolution rate to the formation of metal-deficient polysulfide surface layers, which formed during an initially rapid leaching period. Lu et al. (2000) studied the effect of chloride ions on the dissolution of chalcopyrite in acidic solutions under atmospheric pressure conditions. They showed that in the presence of chloride ions in solution, iron initially dissolves at a faster rate than copper. Parker et al. (2003) conducted microbial leaches at 50 and 65ºC on massive chalcopyrite using *Sulfobacillus thermosulfidooxidans* to study the acidic oxidative dissolution. XPS was also used to characterize surface reaction intermediates and products.

These studies provide considerable insight into factors affecting dissolution of minor sulphides. However, we stress the need to study the dissolution kinetics of galena, sphalerite and chalcopyrite in an attempt to propose a dissolution rate law that accounts for the factors governing the chemical interactions between these sulphides and aqueous solutions. A dissolution rate law accounting for the effects that reactive surface area, aqueous oxygen and protons could exert on the sulphide dissolution reactions has not yet been proposed. A rate law applicable to dissolution of sulphides at constant temperature could be written as (Domènech et al., 2002a; McKibben, 1984):

$$Rate = k_+ \cdot S_{min} \cdot [O_2(aq)]^n \cdot (a_{H^+})^m \quad (1)$$

where Rate is in mol m^{-2} s^{-1}, k_+ is the dissolution rate constant, S_{min} is the reactive surface area, $[O_2(aq)]$ and $(a_{H^+})$are the concentrations of dissolved oxygen and protons, respectively, and n and m are empirical factors. The estimation of the sulphide dissolution rates in the laboratory under conditions that match those in the field, e.g., acidic pH and oxic conditions is a first step towards the elaboration of a rate law. The use of flow-through experiments allows us to study the effects that the different kinetic factors involved in the reaction exert on the dissolution rate.

In the present study we sought (1) to obtain the steady-state dissolution rates of pure sulphides (galena, sphalerite and chalcopyrite) at pH 3 and oxygen saturated atmosphere and 25ºC with non-stirred flow-through experiments, and (2) to compare these rates with the dissolution rates of the minor sulphides making up the Aznalcóllar pyritic sludge under the same conditions. The results obtained form the basis for future experiments designed to fully characterize the complex mechanism accounting for the dissolution of these minor sulphides, and to propose the dissolution rate laws as expressed in eq. (1).

EXPERIMENTAL METHODOLOGY

Sample characterization

The pyritic sludge from the Aznalcóllar mine consists of 73 wt. % of pyrite (FeS_2), 10 wt. % of chlorite, 8 wt. % of quartz, 6 wt. % of gypsum, 1.4 wt. % of sphalerite (ZnS), 0.8 wt. % of galena (PbS) and 0.6 wt. % of chalcopyrite ($CuFeS_2$). It is rich in Fe (36.44 wt. %) and the amounts of potentially toxic elements such as Zn, Pb and Cu are 0.9, 0.7 and 0.2 wt. %, respectively (Domènech et al., 2002). The BET-determined surface area was 1.4 ± 0.2 $m^2\ g^{-1}$ using 5-point N_2 adsorption isotherms. The temperature of sample degassing was 125°C for 20 min. The BET surface area for each sulphide was estimated from correcting the BET value of the sludge by the relative density between each phase and the sludge, yielding the following specific surface areas ($m^2\ g^{-1}$): 1.1 ± 0.2 (pyrite), 0.7 ± 0.2 (galena), 1.4 ± 0.2 (sphalerite) and 1.2 ± 0.2 (chalcopyrite).

Samples of galena, sphalerite and chalcopyrite used in the present study are from El Molar (Catalonian Coastal Range), Vall de Liat (Val d'Aran Pyrenees) and Martinet de Cerdanya (Catalan Pyrenees), respectively. The XRD powder patterns of the galena sample showed that the sample mainly consists of galena (PbS) and approximately 10 wt. % of cerussite ($PbCO_3$) phases. The XRD powder patterns of the sphalerite and chalcopyrite samples showed that the samples are composed of the pure sulphide. Raw samples were ground in an agate mortar and pestle to obtain powder fraction between 10 and 100 μm. SEM images of the initial powder fraction are shown in Fig. 1. The samples were not subject to additional pre-treatments. The BET-determined initial surface area of the galena, sphalerite and chalcopyrite were 0.30 ± 0.03, 0.25 ± 0.02, and 0.44 ± 0.04 $m^2\ g^{-1}$ using 5-point N_2 adsorption isotherms. To purge impurities and allow water evaporation prior to analysis, the sample was degassed at 125°C for 20 min.

Experimental setup

Flow-through experiments were carried out using flow-through Lexan reactors (ca. 35 mL in volume) immersed in a water-bath at 25 ºC ± 0.1 (Fig. 2). The reaction cells were composed of two chambers, a lower chamber with an inner diameter of 33 mm and an upper chamber with an inner diameter of 26 mm. The two chambers were separated by a fine (5μm pore size) nylon mesh, on which sulphide powder was placed. Preliminary experiments showed that the sludge dissolution was not affected by stirring the sample. Therefore, only non-stirred flow-through experiments were used to determine the steady-state dissolution rates of the sulphides. In the flow-through experiments, once the steady state was attained, the dissolution rate, R, (mol $m^{-2}\ s^{-1}$) was calculated based on the release of metal (Fe, Pb, Zn or Cu) and S according to the expression (Nagy et al., 1991)

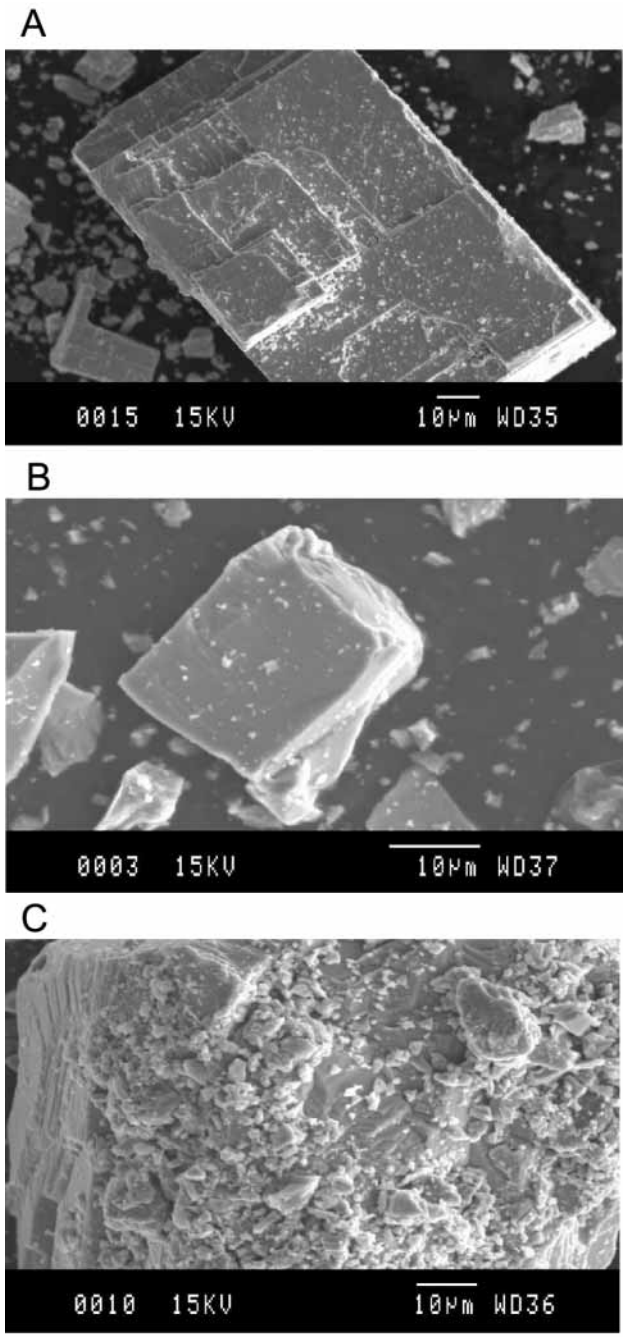

FIGURE 1 **SEM images of the different sulphide samples. A) galena. B) sphalerite. C) chalcopyrite. Microparticles are visibly attached onto the grain surfaces of the sulphides.**

$$\nu_j R = \frac{q}{A}(C_{j,out} - C_{j,inp}) \quad (2)$$

where $C_{j,inp}$ and $C_{j,out}$ are the concentrations of component j (metal or S) in the input and the output solutions,

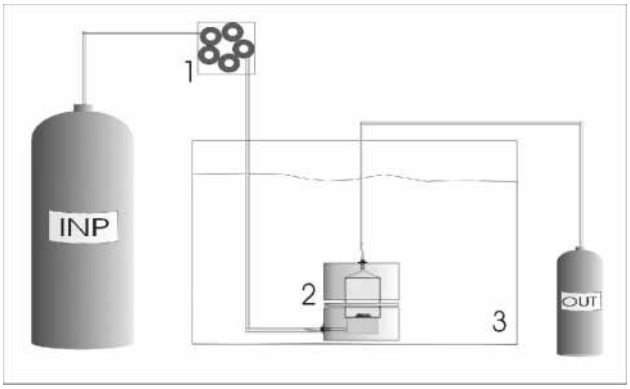

FIGURE 2| **Experimental setup: (1) peristaltic pump; (2) non stirred flow-through reactor immersed in the water bath; (3) water–bath held at constant temperature (25 ± 0.1ºC).**

respectively (mol m^{-3}), v_j is the stoichiometry coefficient of j in the dissolution reaction, A is the reactive surface area (m^2) and q is the fluid volume flux through the system (m^3 s^{-1}). The error in the calculated dissolution rates is approximately 15% and is estimated using the Gaussian error propagation method (Barrante, 1974) from the equation:

$$\Delta R = \left(\left(\frac{C_{j,out}}{A v_j} \right)^2 \cdot \Delta q^2 + \left(\frac{q C_{j,out}}{A^2 v_j} \right)^2 \cdot \Delta A^2 + \left(\frac{q}{A v_j} \right)^2 \cdot \Delta C_{j,out}^2 \right)^{0.5} \quad (3)$$

Solutions

Input solutions at pH 3 were prepared with Millipore MQ water (18 MΩ·cm) and analytical-grade HCl reagent (Merck) and were equilibrated with a constant O_2 partial pressure of 0.20 ± 0.01 atm by means of Alphagaz bottles for 12 h. Total concentrations of Fe, S, Pb, Cu, and Zn of input and output solutions were analysed with ICP-AES and with ICP-MS when the output concentrations of Pb, Cu and Zn were lower than 1 μM. Input and output solution pH was measured with a Crison© combined glass electrode at room temperature (22 ± 2 ºC).

RESULTS AND DISCUSSION

Dissolution of the pyritic sludge

The variation of output concentrations of Fe, Pb, Zn, Cu and S as a function of time is shown in Fig. 3. The experiment consisted of three stages in which the flow rate was changed after the Fe and S output concentrations reached steady state (Fig. 3A). In the first stage the Fe and S released decreased gradually to attain steady state after 300 h approximately. Achievement of steady state was verified by a series of constant Fe output concentrations that differed by less than 5%. Thereafter, as the flow rate was increased, a slight increase in Fe and S was observed in the beginning of the second stage. The output concentrations also decreased until steady state was attained, and the flow rate was changed. Likewise, in the third stage, a slight increase in the Fe and S release was observed before steady state was achieved. The steady-state experimental conditions are listed in Table 1. Whereas the Fe release is due to pyrite dissolution, the release of Pb, Zn and Cu is caused by the dissolution of the small amounts of galena, sphalerite and chalcopyrite (0.8 wt. %, 1.4 wt. % and 0.6 wt. %, respectively) making up the pyritic sludge. The variation of the output concentrations of Pb, Cu and Zn as a function of time is shown in Fig. 3B.

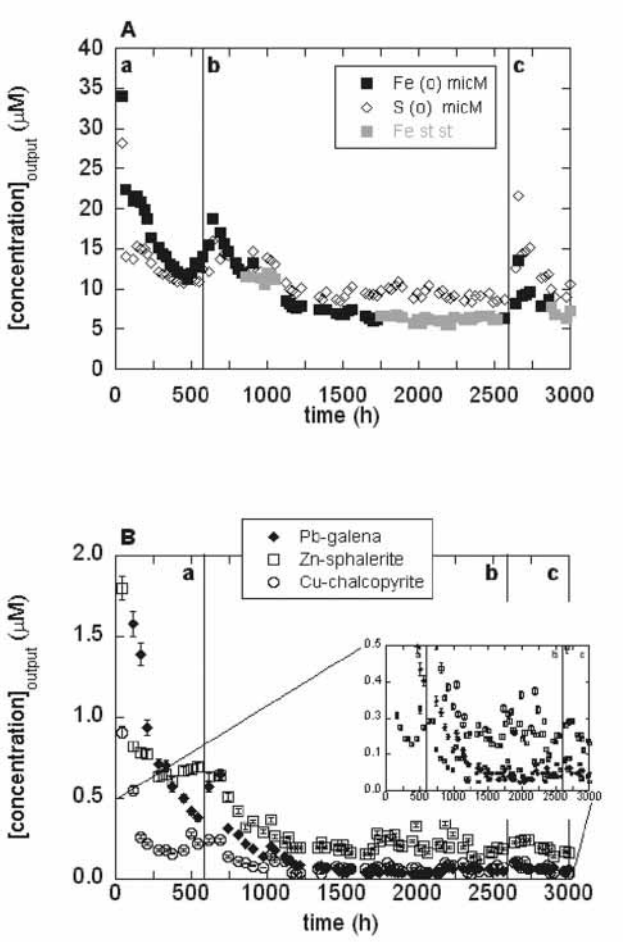

FIGURE 3| **Variation in the output concentrations of the distinct metals and S as a function of time in the experiment with pyritic sludge at pH 3. A) Fe and S associated with pyrite dissolution. B) Pb, Zn and Cu associated with the dissolution of galena, sphalerite and chalcopyrite. The grey solid symbols denote concentration values used to calculate average steady state. In stage b the grey symbols represent an early steady-state condition between 750 and 1000 h. The vertical lines represent changes in flow rate between the different stages (a: 0.050; b: 0.122 and c: 0.075 mL min^{-1}, respectively).**

TABLE 1 | **Steady-state experimental conditions in the flow-through experiments.**

sludge-expts.	expt. run (h)	flow rate (ml min^{-1})	pH input	pH output	metal output	(µM)	S output	(metal/S)	final mass (g)	surface (m^2g^{-1})	R metal (mol $m^{-2}s^{-1}$)
sludge-25-pyrite-b	2520	0.122	2.89	2.92	Fe	6.38	8.91	0.7	0.127	1.1	$9.16\pm1.39\times10^{-11}$
sludge-25-pyrite-c	3046	0.075	2.89	2.92	Fe	6.98	10.18	0.7	0.125	1.1	$6.33\pm0.96\times10^{-11}$
sludge-25-galena-b	2520	0.122	2.99	3.02	Pb	0.05		-	0.0011	0.7	$1.22\pm0.18\times10^{-10}$
sludge-25-galena-c	3046	0.075	2.99	3.01	Pb	0.06		-	0.0010	0.7	$1.08\pm0.16\times10^{-10}$
sludge-25-sphalerite-b	2500	0.122	2.89	2.93	Zn	0.08		-	0.0025	1.4	$4.89\pm0.73\times10^{-11}$
sludge-25-sphalerite-c	3046	0.075	2.89	2.93	Zn	0.08		-	0.0025	1.4	$2.92\pm0.43\times10^{-11}$
sludge-25-chalcopyrite-b'	1989	0.128	2.97	3.00	Cu	0.03		-	0.0011	1.2	$5.11\pm0.77\times10^{-11}$
sludge-25-chalcopyrite-b	2500	0.122	2.89	2.93	Cu	0.03		-	0.0011	1.2	$4.48\pm0.67\times10^{-11}$
mineral-expts.											
galena-25-1-a	1676	0.028	3.00	2.83	Pb	23.77	6.26	3.8	0.222	0.3	$1.69\pm0.25\times10^{-10}$
galena-25-1-b	2539	0.087	3.00	3.01	Pb	4.65	*1.29*		0.216	0.3	$1.04\pm0.16\times10^{-10}$
galena-25-1-c	3381	0.013	3.00	3.06	Pb	33.94	8.35	4.1	0.212	0.3	$1.17\pm0.18\times10^{-10}$
sphaZn-25-1-a	1651	0.036	3.00	2.81	Zn	3.05	*1.53*	-	0.248	0.3	$2.93\pm0.44\times10^{-11}$
sphaZn-25-1-b	2515	0.089	3.00	2.90	Zn	1.02	*0.36*	-	0.247	0.3	$2.47\pm0.37\times10^{-11}$
sphaZn-25-1-c	3307	0.014	3.00	3.00	Zn	3.46	2.89	1.2	0.247	0.3	$1.30\pm0.19\times10^{-11}$
chalcopyrite-25-1-a	1630	0.034	3.00	2.95	Cu	5.19	6.08	0.9	0.247	0.4	$2.70\pm0.41\times10^{-11}$
chalcopyrite-25-1-b	2492	0.087	3.00	2.93	Cu	1.28	*0.79*	-	0.246	0.4	$1.71\pm0.26\times10^{-11}$

S output values in italics **indicate that the measured concentration is close or lower to the detection limit (1.5µM).**
Stoichiometric ratio indicated as "-" means no calculated since S output concentration was not measured or below detection limit.
Metal and sulphur input concentrations are 0 µM.

The stoichiometric ratio (SR*i/j*) between two components is defined as the ratio between the release of *i* and the release of *j*:

$$SR_{i/j} = \frac{C_{i,out} - C_{i,inp}}{C_{j,out} - C_{j,inp}} \quad (4)$$

where $C_{i,inp}$ and $C_{i,out}$ are the concentrations of component *i* in the input and the output solution, respectively. During the entire experiment, the ratio Fe/S was always higher than the expected Fe/S ratio (0.5) (Fig. 4) since total Fe release and 95 % of the total S release were from pyrite dissolution (73 wt. % of the sludge). In the first few hours, the Fe/S ratio showed a sharp increase up to 1.65. Then, the Fe/S ratio started decreasing gradually down to 1.2 in the first steady state and 0.7 in the second and third steady states. This relative lack of total aqueous sulphur might be due to the precipitation of secondary sulphur-phases (anglesite, cerussite, native sulphur, gypsum and barite). The degree of saturation of the output solutions with respect to these sulphur-bearing phases is calculated using the EQ3NR code (Wolery, 1992). Calculations show that the output solutions are highly undersaturated with respect to the mentioned sulphur-phases throughout the experimental run. Hence, precipitation could be ruled out as a possible mechanism responsible for the depletion of total aqueous sulphur. Secondly, in the first 1000 h the Fe/S ratio was very high (up to 1.65) (see Fig. 4). Although an initial dissolution of highly reactive pyritic microparticles can account for the non-stoichiometric dissolution, the lack of aqueous sulphur throughout the experimental run may be explained by fast dissolution of chlorite (10 wt. % of the sludge) at pH 3, which results in an extra release of Fe to solution (Domènech et al., 2002). As the chlorite continued dissolving, the Fe/S ratio diminished to a steady average value of 0.70 ± 0.05, which was still higher than the ideal one (0.5). The stoichiometric Pb/S, Zn/S and Cu/S ratios

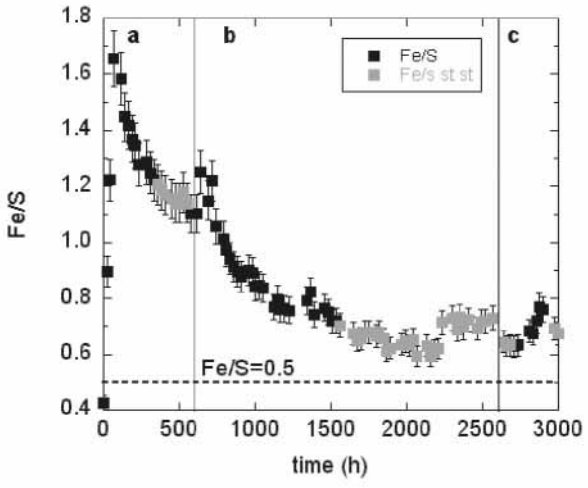

FIGURE 4 | **Variation in the stoichiometric Fe/S ratio as a function of time in the flow-through experiment with pyritic sludge. Grey solid symbols correspond to steady state. The dotted line shows the ideal Fe/S ratio (0.5). The vertical lines represent changes in flow rate between the different stages (a: 0.050; b: 0.122 and c: 0.075 mL min^{-1}, respectively).**

were not calculated given that the major sulphur released was from pyrite dissolution.

Based on the release of Fe, the steady-state dissolution rate of pyrite ($Rate_{Fe}$) is 6.33 ± 0.96 x 10^{-11} mol m^{-2} s^{-1} according to the rate determined at the end of stages B and C (Fig. 3A). Domènech et al. (2002) obtained a pyrite dissolution rate of 1.0 x 10^{-10} mol m^{-2} s^{-1}, which is 1.6 times faster than the one estimated in the present study. This difference may be attributed to the fact that these authors considered the attainment of steady state before 1000 h, yielding a faster dissolution rate. This is supported by considering an early steady-state condition between 750 and 1000 h in the present study (see Fig. 3A). Based on the release of Pb, Zn and Cu, the steady-state dissolution rates of galena ($Rate_{Pb}$), sphalerite ($Rate_{Zn}$) and chalcopyrite ($Rate_{Cu}$) are 1.1 ± 0.16 x 10^{-10}, 2.92 ± 0.43 x 10^{-11} and 4.48 ± 0.67 x 10^{-11} mol m^{-2} s^{-1}, respectively. Hence, it is observed that as pyritic sludge dissolves at pH 3, galena dissolves 1.6, 2.2 and 3.4 times faster than pyrite, chalcopyrite and sphalerite, respectively.

Dissolution of galena, sphalerite and chalcopyrite

The non-stirred flow-through experiments of dissolution of galena, sphalerite and chalcopyrite were performed independently at pH 3. The experiments for dissolution of galena and sphalerite consisted of three stages and lasted for almost 3500 h, whereas the experiment with chalcopyrite dissolution consisted of two stages and lasted 2500 h. During the experimental run, the flow rate was changed (0.013 to 0.089 ml min^{-1}) after steady state was reached. The variation of the output concentrations of Pb, Zn, Cu, Fe and S as a function of time in the respective experiments is plotted in Fig. 5. Steady state in each stage lasted at least 100 h and was verified by a series of constant output concentrations that differed by less than 5%. In the beginning of a new stage, the output concentrations showed a slight increase. Details of the steady-state experimental conditions are given in Table 1. A persistent smell of $H_2S_{(g)}$ was noted when the output solutions were collected. The output pH values were (within error) the same as the initial pH (3 ± 0.06) in the three experiments. Based on the Pb, Zn, Fe, Cu and S output concentrations, the saturation states of the output solutions were calculated using the EQ3NR code (Wolery, 1992) at pH 3 and 25ºC. Calculations show that dissolution took place under highly undersaturated conditions with respect to pyrite, galena, anglesite, cerussite, sphalerite, chalcopyrite and native sulphur.

Given that it was not possible to measure the BET surface areas for the recovered samples, the dissolution rates were normalized to initial BET surface areas. We assume that the initial BET surface area and the reactive surface

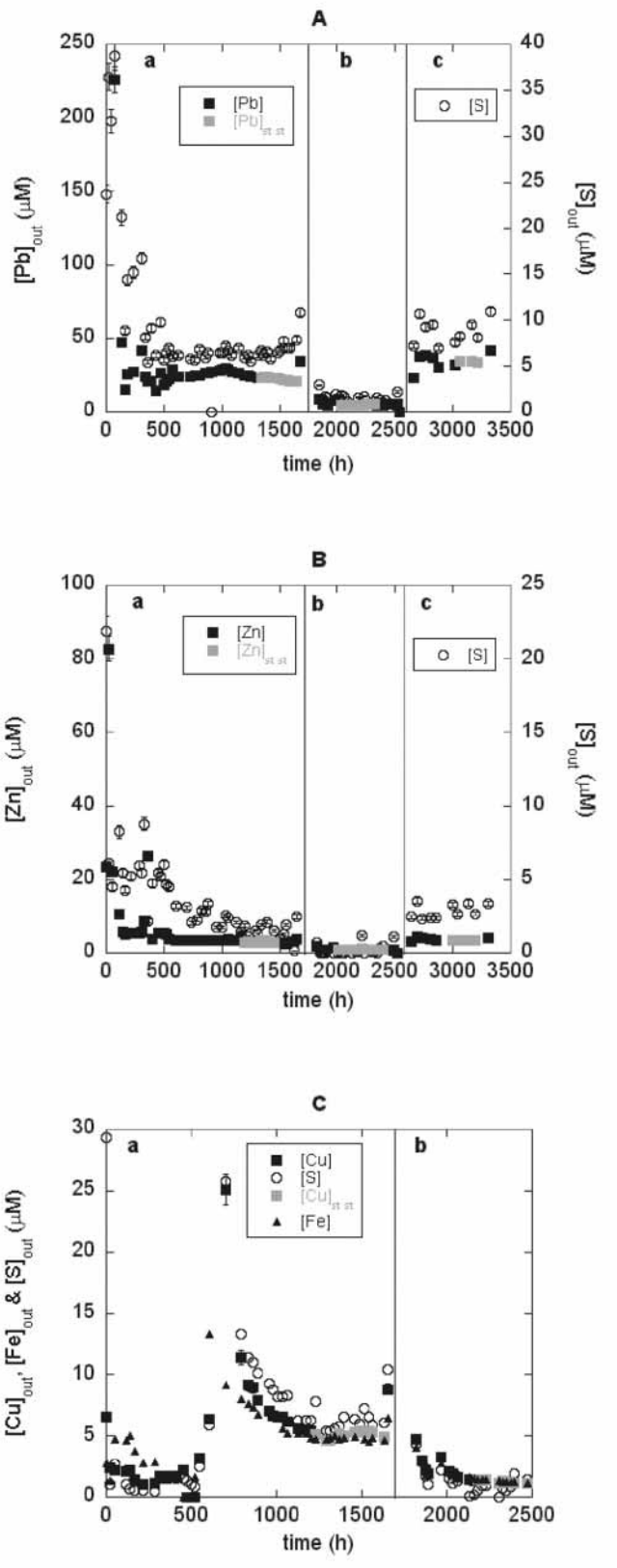

FIGURE 5 **Variation in the output concentrations of Pb, Zn, Cu and S as a function of time in the flow-through experiments at pH 3. A) galena. B) sphalerite. C) chalcopyrite. The grey solid symbols denote values of metal output concentrations used to calculate average steady state. Vertical lines denote the different stages based on the changes of flow rate (see Table 1).**

area are identical bearing in mind that the reactive surface area correlates linearly with the BET surface area and that this correlation is independent of temperature and pH (Ganor et al., 1995). The normalization of the dissolution rate with the initial BET surface area is a prior step to the determination of the influence of the final surface area on the calculation of the steady-state dissolution rates of the sulphides with eq. (2). The use of the BET surface area as a proxy of reactive surface area is open to debate (Nagy et al., 1991; Hodson, 1998; Brantley and Mellott, 2000; Prenat and Oelkers, 2000; Metz and Ganor, 2001; Brandt et al., 2003 and references herein). Ongoing experiments conducted with larger amounts of sample to ensure measurements of the final BET specific surface area, will provide results to account for the sulphide dissolution rates obtained in the present study.

Dissolution of PbS

The release of Pb and S sharply increased at the beginning of the experiment. Subsequently, the output concentrations decreased to approach steady state (Fig. 5A). It is likely that the high initial dissolution of galena is caused by fast dissolution of microparticles, which originated from sample grounding and fast dissolution of cerussite at pH 3. The output S concentration was lower than that of output Pb so that the stoichiometric Pb/S ratio was considerably higher than the ideal Pb/S ratio of 1, reaching a value of 4 ± 0.25 at steady state (Fig. 6a). This relative lack of aqueous sulphur is discussed below. In stage B, the Pb/S ratio was not calculated because the S output concentrations were below the detection limit. Owing to such a sulphur deficit in the dissolution of galena, the dissolution rate was calculated based on Pb release ($Rate_{Pb}$). Based on the steady-state rates obtained at each stage, where the flow rate was changed, the average galena dissolution rate is $1.20 \pm 0.18 \times 10^{-10}$ mol m^{-2} s^{-1} at pH 3.

Dissolution of ZnS

A similar pattern of release of Zn and S was observed for the sphalerite dissolution: first, a high release of Zn and S within 100 h and then a decrease in Zn and S concentrations until steady state was achieved. The steady state achievement was after 1000 h in the first stage (Fig. 5B). After changing the flow rate, steady state was attained in stages B and C. In stage A the stoichiometric ratio Zn/S was nearly 1 in the first 500 h and increased up to 1.7 ± 0.15 until stage B was initiated. In stage B, the Zn/S ratio was not taken into account since the S output concentrations were below the detection limit. In stage C, the stoichiometric ratio was 1.2 ± 0.1 (Fig. 6B). Owing to sulphur depletion in the flow-through experiments, the dissolution rate was calculated based on the Zn release ($Rate_{Zn}$). The calculated steady-state rates in stages A and B were the same within error but higher than that in stage

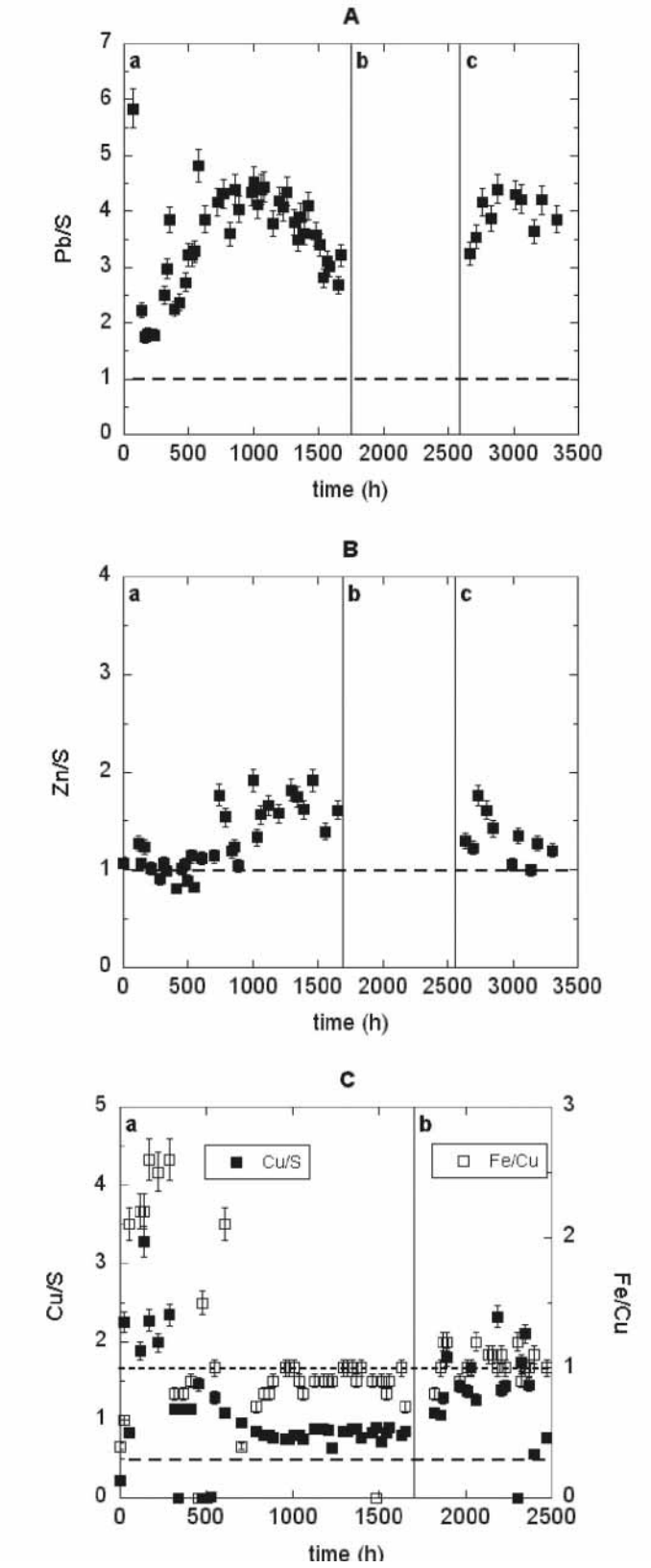

FIGURE 6 **Variation in the stoichiometric ratios of Pb/S, Zn/S and Cu/S and Cu/Fe as a function of time in the flow-through experiments at pH 3. A) galena. B) sphalerite. C) chalcopyrite. The dashed lines denote the respective ideal stoichiometric ratio (Pb/S, Zn/S and Cu/S), and the dotted line in (C) represents the stoichiometric Fe/Cu ratio of chalcopyrite.**

TABLE 2 | **Comparison of the sulphide dissolution rates (mol m^{-2} s^{-1}).**

		flow-through			leach experiment	batch experiment		
mineral	**rate**	**sludge(1)**	**sludge(2)**	**single sulphide(1)**	**single sulphide(3)**	**single sulphide(4)**		
pyrite	$Rate_{Fe}$	$6.33x10^{-11}$	$1.00x10^{-10}$			pH 0.43	pH 0.93	pH 1.42
galena	$Rate_{Pb}$	$1.08x10^{-10}$	$2.80x10^{-10}$	$1.20x10^{-10}$		$7.33x10^{-8}$	$4.40x10^{-8}$	$8.05x10^{-9}$
sphalerite	$Rate_{Zn}$	$2.92x10^{-11}$	$4.00x10^{-11}$	$1.30x10^{-11}$	$1.14x10^{-9}$			
chalcopyrite	$Rate_{Cu}$	$4.48x10^{-11}$	$8.00x10^{-11}$	$1.71x10^{-11}$				

(1)**present study at pH 3 using flow-through experiments.** (2)**Domènech et al. (2002a) at pH 3.** (3)**Weisener et al. (2003) at pH 1.** (4)**Zhang et al. (2004) at pH 0.43-1.42.**

C (Table 1) probably caused by a decrease in particle reactivity. In this case, the sphalerite dissolution considered at pH 3 was $1.30 \pm 0.19 \times 10^{-11}$ mol m^{-2} s^{-1}.

Dissolution of $CuFeS_2$

The release of Cu, Fe and S was high at the onset of the experiment probably due to the fast dissolution of microparticles. In stage A, the steady state was attained after 750 h because of flow rate instability. Thereafter, the release of Cu, Fe and S decreased and, steady state was attained (Fig. 5C). Until 750 h, the stoichiometric ratios Cu/S and Fe/Cu were higher than 0.5 and 1, respectively. Subsequently, at steady state the Cu/S and Fe/Cu ratios were 0.90 ± 0.05 and 0.95 ± 0.05, respectively (Fig. 6C). In stage B, the Cu/S ratio was also higher than 0.5 and the Fe/Cu ratio was about one. Overall, when chalcopyrite dissolved, the dissolution resulted in a significant sulphur deficit and, at steady state, the concentration of Cu with respect to Fe was close to stoichiometry. Based on Cu release and considering the last steady-state, the dissolution rate of chalcopyrite ($Rate_{Cu}$) at pH 3 was $1.71 \pm 0.26 \times 10^{-11}$ mol m^{-2} s^{-1} (stage B).

Comparison of the sulphide dissolution rates

The steady-state dissolution rate of galena is faster than those of chalcopyrite and sphalerite ($Rate_{Pb} > Rate_{Cu} \approx Rate_{Zn}$) using the pure sulphide sample as starting material. This is consistent with the measured rates in Rimstidt et al. (1994), who studied the catalytic effect of ferric iron on the sulphide dissolution at pH 2 and showed that galena dissolves faster than sphalerite and chalcopyrite. Moreover, using the pyritic sludge from Aznalcóllar as starting material, the dissolution rate of galena is faster than that of pyrite, chalcopyrite and sphalerite ($Rate_{Pb} > Rate_{Fe} > Rate_{Cu} \approx Rate_{Zn}$) (see Table 2). The two measured rates of galena are the same within error, regardless of the type of sample. The dissolution rates of chalcopyrite and sphalerite in the sludge are a factor of 2.6 and 2.3 faster, respectively, than those for the sulphides alone.

Weisener et al. (2003) reported a dissolution rate of sphalerite at pH 1 and 25ºC faster than the one obtained in the present study at pH 3 (Table 2). Zhang et al. (2004) also reported faster galena dissolution rates at pH ranging from 0.43 to 1.42 than the rate obtained in the present study at pH 3. On the assumption that the dissolution reactions of sphalerite and galena are proton promoted in the respective pH ranges, and according to the empirical equation (Wieland et al., 1988)

$$Rate = k_{H^+} \cdot a_{H^+}^{n_{H^+}} \quad (5)$$

where a_{H+} is the activity of protons in the solution, n_{H+} is the order of the reaction with respect to H^+ and k_{H+} is a rate coefficient, the calculated order of the reaction, n_{H+}, is 0.97 for sphalerite and 1.12 ± 0.09 for galena. Although the n_{H+} value for sphalerite is only based on one rate at pH 1 and at pH 3 (Weisener et al., 2003) and present study), this suggests a strong dissolution rate-pH dependency. Likewise, galena dissolution shows a high dependence on pH. These high $n_{H_{H+}}$values contrast with the low value of the reaction order of 0.11 ± 0.01 (Williamson and Rimstidt, 1994) and 0.1 ± 0.08 (Domènech et al., 2002a) for pyrite dissolution.

The longevity of the sulphide particles can be estimated assuming a spherical form (Lengke and Temple, 2002). According to the dissolution rates of the sulphides obtained in the present study, we can calculate the approximate time for a 1-mm radius sphere of pyrite, galena, sphalerite and chalcopyrite to dissolve based on the following equation (Lasaga, 1998)

$$t_{lifetime} = \frac{r_0}{k_+ \cdot \bar{V}} \quad (6)$$

where r_0 is the initial radius of a spherical particle (cm), k_+ is the dissolution rate constant (mol cm^{-2} s^{-1}) at the determined solution pH, and $\bar{V}$ is the molar volume of the mineral (cm^3 mol^{-1}). Hence, at pH 3, oxygen saturated conditions and 25ºC and the molar volumes of galena (31.49), pyrite (23.94), sphalerite (23.83) and chalcopyrite (42.83), the respective lifetime is 10, 21, 100 and 43 ($x10^3$) years.

Stoichiometry of the dissolution reactions

In acidic pH and in the presence of dissolved oxygen, the galena decomposition can be represented by two major overall reactions:

$$PbS(s) + 2H^+ \leftrightarrow Pb^{2+} + H_2S(aq) \quad (7)$$

$$PbS(s) + 2O_2(aq) \leftrightarrow Pb^{2+} + SO_4^{2-} \quad (8)$$

Reaction (7) is the dissolution of galena and reaction (8) is the oxidation of galena. Subsequently, aqueous oxygen oxidizes the sulphydric (H_2S(aq)) to sulfate (SO_4^{2-}):

$$H_2S(aq) + 2O_2(aq) \leftrightarrow 2H^+ + SO_4^{2-} \quad (9)$$

The overall stoichiometry would result in a stoichiometric Pb/S ratio (S represents total aqueous sulphur) of 1.

However, the experiments described above lead to an excess of metal, reaching Pb/S values of 4 ± 0.25. The lack of stoichiometry may be attributed to the precipitation of elemental sulphur. De Giudici and Zuddas (2001) conducted in situ AFM experiments to study the galena dissolution at pH ≤ 3, and observed protrusions formed on the galena surface, which were composed of native sulphur. This intermediate and slowly dissolving phase would react with oxygen to dissolve and migrate towards bulk solution in a more oxidised state (e.g. as SO_4^{2-} or $S_2O_3^{2-}$). Although the resolution is not as powerful as that of AFM, the SEM photographs of the recovered samples of galena that underwent dissolution showed no evidence of elemental sulfur on the grain surfaces (Fig. 7A).

An alternative explanation for the Pb/S ratios higher than 1 could be the loss of H_2S(aq) via gasification whereby H_2S(aq) partially converts to H_2S(g):

$$H_2S(aq) \rightarrow H_2S(g) \quad (10)$$

This is supported by the intense H_2S(g) smell noted during collection of the output solutions.

The amounts of H_2S(aq) and SO_4^{2-} produced in solution depend on the relative concentrations of protons and

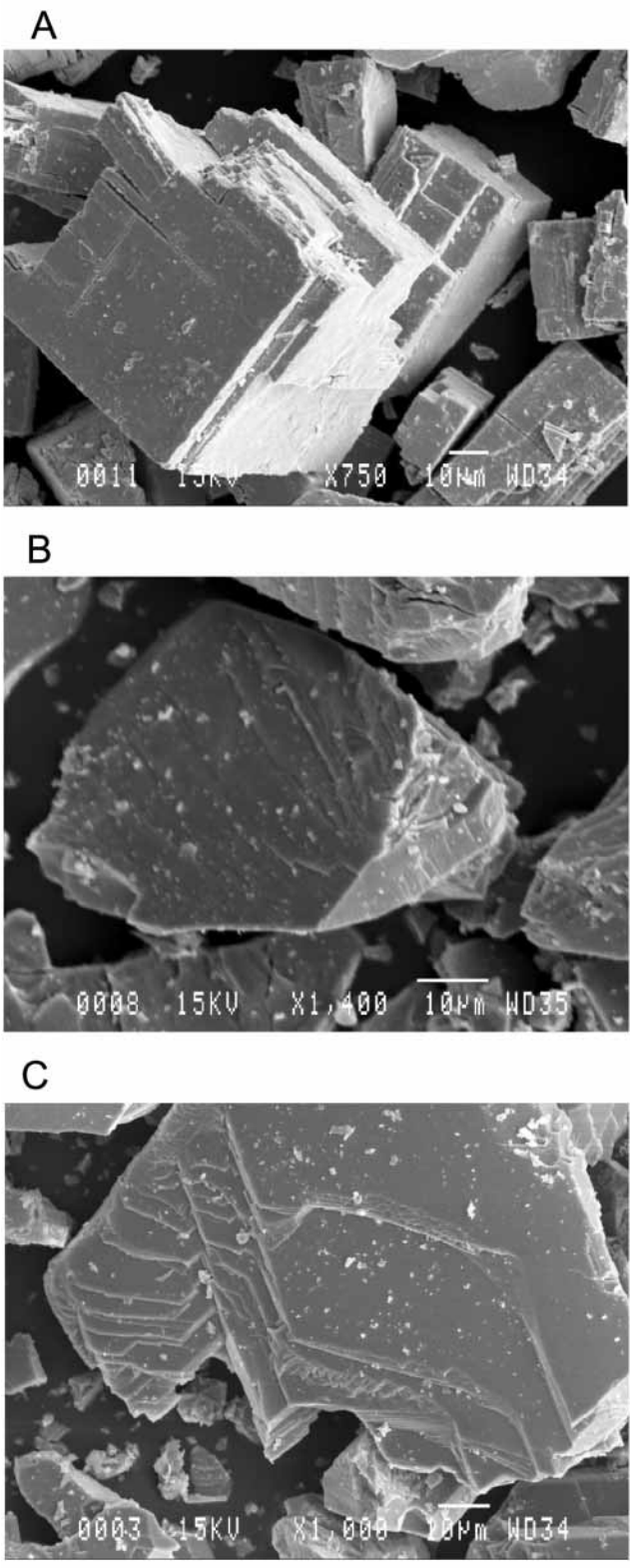

FIGURE 6| **SEM photographs of the sulphides after the experiment. Sulphur precipitation is not observed. A) Microparticles mostly dissolved on the galena grains, which present smooth faces. B) The sphalerite grains show steps formed by dissolution. C) the chalcopyrite grains show typical features of dissolution at the edges and remains of dissolved layers.**

dissolved oxygen given that protonation and oxidization of galena can occur in parallel (reactions 7 and 8). At pH 3, proton concentration (~10^{-3} M) is higher than the concentration of dissolved oxygen (2.5 x 10^{-4} M), and adsorption of protons occurs preferentially against oxygen adsorption, resulting in a significant production of H_2S(aq) and a low production of SO_4^{2-}. This agrees with the reaction model reported in Hsieh and Huang (1989), where protons are adsorbed on the negatively charged surface of galena, and the resulting protonated surface sites ($PbSH_4^{2+}$ (s)) act as intermediate species before release of lead and sulphur to the solution. An increase in solution pH would result in a decrease in proton concentration, reaction (8) would proceed faster than reaction (7) and the amount of sulfate produced would increase and overcome the amount of H_2S(aq) at certain pH. Therefore, the Pb/S ratio would not be representative of the dissolution stoichiometry, i.e., that one atom of Pb and one atom of S are released to the solution following breakage of the PbS structure.

As for sphalerite dissolution, the Zn/S ratio at steady state (1.2 ± 0.1) almost matched the stoichiometric value, yielding a small deficit in aqueous sulphur. It is possible that the Zn/S ratio obtained results from an overestimation of the S concentration owing to an analytical error associated with the measurement of low sulphur concentrations. Ignoring this and assuming that the measured sulphur is the true concentration of aqueous sulphur, H_2S(aq) was not the predominant sulphur species at pH 3. Nevertheless, there is a need for further experiments designed to guarantee larger sulphur concentrations to reduce the analytical uncertainty in order to better quantify the expected sulphur deficit. As in the case of galena, no elemental sulphur was detected on the dissolved sphalerite surface (Fig. 7B).

Chalcopyrite dissolution at pH 3 also yielded a significant deficit of total aqueous sulphur (Cu/S = 0.90 ± 0.05) with respect to the stoichiometric ratio of 0.5. This value indicates that oxidization and protonation take place simultaneously. Precipitation of elemental sulphur was not observed in the SEM photographs of the reacted sample (Fig. 7C). An interesting finding is that the Cu/Fe ratio is 0.95 ± 0.05, which suggests that chalcopyrite dissolves stoichiometrically according to the framework metals of this sulphide. Further flow-through experiments with these sulphides at different reacting pH, especially at pH values higher than 3 (with lower proton concentrations) should be carried out to conform the above observation.

With respect to pyrite, the study of its dissolution falls beyond the scope of the present study. The deficit of total sulphur during the dissolution of the pyritic sludge (Fe/S= 0.7) cannot be solely attributed to a possible sulphur deficit. In this case, the dissolution of chlorite (10 wt. % of the sludge) at pH 3 causes an additional release of iron to solution and thus an increase in the stoichiometric Fe/S ratio as pointed out by Domènech et al. (2002a).

CONCLUSIONS

The steady-state dissolution rate constants of galena, sphalerite and chalcopyrite at pH 3 and oxygen saturated conditions (P_{O_2} = 0.21 atm) were obtained based on the release of Fe, Pb, Zn and Cu using non-stirred flow-through experiments at 25 ± 0.1ºC. These rate constants, normalized to the initial BET surface areas, are 1.2 ± 0.18 x 10^{-10}, 1.30 ± 0.19 x 10^{-11} and 1.71 ± 0.26 x 10^{-11} mol m^{-2} s^{-1} for galena, sphalerite and chalcopyrite using raw sulphide samples as starting materials. Therefore, galena dissolution rate is approximately one order of magnitude faster than that of chalcopyrite and sphalerite at pH 3 and oxygen saturated at 25ºC.

From the dissolution of pyritic sludge, the steady-state dissolution rates of pyrite, galena, sphalerite and chalcopyrite are 6.33 ± 0.96 x 10^{-11}, 1.10 ± 0.16 x 10^{-10}, 2.92 ± 0.43 x 10^{-11} and 4.48 ± 0.67 x 10^{-11} mol m^{-2} s^{-1}, respectively. Thus, galena dissolves 1.6, 2.2 and 3.4 times faster than pyrite, chalcopyrite and sphalerite, respectively. The galena dissolution rate is the same using raw galena as starting material or a pyritic sludge sample from Aznalcóllar, which contains 0.8 wt. % of galena. The dissolution rates of sphalerite and chalcopyrite are slightly slower using raw sulphide than using the pyritic sludge as starting material.

We suggest that protonation and oxidization could be the two processes involved in the overall mechanism of dissolution of galena, sphalerite and chalcopyrite. Predominance of the former over the latter could depend on pH. At pH 3, galena dissolution is mostly governed by protonation, whereas dissolution of sphalerite and chalcopyrite is substantially controlled by oxidation. The sulphur deficit in the output solutions is due to a significant loss of aqueous sulphur as the reaction product H_2S(aq) rapidly converts to H_2S(g). This lack of aqueous sulphur renders the metal/S ratios invalid as indicators of reaction stoichiometry. The Cu/Fe ratio at steady state during chalcopyrite dissolution suggests that chalcopyrite dissolves stoichiometrically.

Although SEM photographs showed the absence of S precipitated on the grain surfaces, formation of elemental sulphur during dissolution cannot be discarded. Further experiments should be conducted at other acidic pH values (with similar concentrations of protons and dissolved oxygen) in order to reinforce the overall mechanism proposed for dissolution of these sulphides.

ACKNOWLEDGEMENTS

This work was partially funded by the European Research project PIRAMID and by a Research and Development contract with the Spanish Government CICYT. JC is also supported by a grant from the Catalan government. We are indebted to Albert Soler who supplied the sulphide minerals. The analytical assistance of Javier Pérez, Rafel Bartrolí, Mercè Cabanes, Sílvia Martínez and Josep Elvira is gratefully acknowledged. The helpful comments of José Luis Mogollón, Javier F. Huertas and an anonymous reviewer have improved the quality of the manuscript.

REFERENCES

Alastuey, A., García-Sánchez, A., López, F., Querol, X., 1999. Evolution of pyrite mud weathering and mobility of heavy metals in the Guadiamar valley after the Aznalcóllar spill, southwest Spain. Science of Total Environment, 242, 41-55.

Ayora, C., Guijarro, A., Domènech, C., Fernández, I., Gómez, P., Manzano, M., Mora, A., Moreno, L., Navarrete, P., Sánchez, M., Serrano, J., 2001a. Actuaciones para la corrección y el seguimiento de la contaminación hídrica. Boletín Geológico y Minero, 112, 123-136.

Ayora, C., Baretitino, D., Doménech, C., Fernández, M., López-Pamo, E., Olivell S., De Pablo, J., Saaltink, M.W., 2001b. Meteorización de los lodos piríticos de Aznalcóllar. Boletín Geológico y Minero, 112, 137-162.

Barrante, J.R., 1974. Applied Mathematics for Physical Chemistry. New Jersey, ed. Prentice-Hall, 256 pp.

Bobeck, G.E., Su, H., 1985. Kinetics of dissolution of sphalerite in ferric chloride solution. Metallurgical Transactions B (Process Metallurgy), 16, 413-424.

Bonissel-Gissinger, P., Alnot, M., Ehrhardt, J.J., Behra, P., 1998. Surface oxidation of pyrite as a function of pH. Environmental Science and Technology, 32, 2839-2845.

Brandt, F., Bosbach, D., Krawczyk-Bärsch, E., Arnold, T., Bernhard, E., 2003. Chlorite dissolution in the acid pH-range: A combined microscopic and macroscopic approach. Geochimica and Cosmochimica Acta, 67, 1451-1461.

Brantley, S.L., Mellott, N.P., 2000. Surface area and porosity of primary silicate minerals. American Mineralogist, 85, 1767-1783.

De Giudici, G., Zuddas, P., 2001. In situ investigation of galena dissolution in oxygen saturated solution: Evolution of surface features and kinetic rate. Geochimica and Cosmochimica Acta, 65, 1381-1389.

Domènech, C., De Pablo, J., Ayora, C., 2002a. Oxidative dissolution of pyritic sludge from the Aznalcóllar mine (SW Spain). Chemical Geology, 190, 339-353.

Domènech, C., Ayora, C., De Pablo, J., 2002b. Sludge weathering and mobility of contaminants in soil affected by the Aznalcóllar tailing dam spill (SW Spain). Chemical Geology, 190, 355-370.

Drever, J.I., 1997. The Geochemistry of Natural Waters. Surface and groundwater environments. New Jersey, ed. Prentice-Hall, 436 pp.

Fornasiero, D., Li, F., Ralston, J., Smart, R.S.C., 1994. Oxidation of galena surfaces. I. X-ray photoelectron spectroscopic and dissolution kinetics. Journal of Colloid and Interface Science, 164, 334-344.

Ganor, J., Mogollón, J.L., Lasaga, A.C., 1995. The effect of pH on kaolinite dissolution rates and on activation energy. Geochimica and Cosmochimica Acta, 59, 1037-1052.

Higgins, S.R., Hamers, R.J., 1996. Chemical dissolution of the galena (001) surface observed using electrochemical scanning tunnelling microscopy. Geochimica and Cosmochimica Acta, 60, 3067-3073.

Hodson, M.E., 1998. Micropore surface area variation with grain size in unweathered alkali feldspars: implications for surface roughness and dissolution studies. Geochimica and Cosmochimica Acta, 62, 3429-3435.

Hsieh, Y.H., Huang, C.P., 1989. The dissolution of PbS(s) in dilute aqueous solutions. Journal of Colloid and Interface Science, 131, 537-549.

Kamei, G., Ohmoto, H., 2000. The kinetics of reaction between pyrite and O_2-bearing water revealed from in situ monitoring of DO, Eh and pH in a closed system. Geochimica and Cosmochimica Acta 64, 2585-2601.

Lasaga, A.C., 1998. Kinetic Theory in the Earth Sciences. Princeton, Princeton University Press, 810 pp.

Lengke, M.G., Tempel, R.N., 2002. Reaction rates of natural orpiment oxidation at 25 to 40ºC and pH 6.8 to 8.2 and comparison with amorphous As_2S_3 oxidation. Geochimica and Cosmochimica Acta, 66, 3281-3291.

Lowson, R.T., 1982. Aqueous oxidation of pyrite by molecular oxygen. Chemical Reviews, 82, 461-497.

Lu, Z.Y., Jeffrey, M.I., Lawson, F., 2000. The effect of chloride ions on the dissolution of chalcopyrite in acidic solutions. Hydrometallurgy, 56, 189-202.

McKibben, M.A., Barnes, H.L., 1986. Oxydation of pyrite in low temperature acidic solutions: Rate laws and surface textures. Geochimica and Cosmochimica Acta, 50, 1509-1520.

Metz, V., Ganor, J., 2001. Stirring effect on kaolinite dissolution rate. Geochimica and Cosmochimica Acta, 65, 3475-3490.

Moses, C.O., Herman, J.S., 1991. Pyrite oxidation at circumneutral pH. Geochimica and Cosmochimica Acta, 55, 471-482.

Nagy, K.L., Blum, A.E., Lasaga, A.C., 1991. Dissolution and precipitation kinetics of kaolinite at 80ºC and pH 3. American Journal of Science, 291, 649- 686.

Nicholson, R.V., Gillham, R.W., Reardon, E.J., 1988. Pyrite oxidation in carbonated-buffered solution: 1. Experimental kinetics. Geochimica and Cosmochimica Acta, 52, 1077-1085.

Nordstrom, D.K., Alpers, C.N., 1999. Geochemistry of acid mine waters. In: Plumlee, G.S., Logsdon M.B. (eds.). The Environmental Geochemistry of Mineral Deposits, Part A: Processes, Techniques, and Health Issues. Colorado, Reviews in Economic Geology, 6A, 133-160.

Parker, A., Klauber, C., Kougianus, A., Watling, H.R., van Bronswijk, W., 2003. An X-ray photoelectron spectroscopy study

of the mechanism of oxidative dissolution of chalcopyrite. Hydrometallurgy, 71, 265-276.

Pashkov, G.L., Mikhlina, E.V., Kholmogorov, A.G., Mikhlin, Y.L., 2002. Effect of potential and ferric ions on lead sulfide dissolution in nitric acid. Hydrometallurgy, 63, 171-179.

Prenat, M., Oelkers, E.H., 2000. Journal of conferences abstracts, Goldschmidt 2000, V. 5(2), 817.

Rimstidt, J.D., Chermark, J.A., Gagen, P.M., 1994. Rates of reaction of galena, sphalerite, chalcopyrite and arsenopyrite with Fe (III) in acidic solutions. In: Alpers, C.N., Bowes, D.W. (eds.). Environmental geochemistry of sulphide oxidation. Washington, D.C., American Chemical Symposium Series 550, 2-13.

Rosso, K.V., Becker, U., Hochella Jr., M.F., 1999. The interaction of pyrite {100} surfaces with O_2 and H_2O: fundamental oxidation mechanisms. American Mineralogist, 84, 1549-1561.

Weisener, G.G., Smart, R.S.C., Gerson, A.R., 2003. Kinetics and mechanisms of the leaching of low Fe sphalerite. Geochimica and Cosmochimica Acta, 67, 823-830.

Wieland, E., Wehrli, B., Stumm, W., 1988. The coordination chemistry of weathering: III. A generalization on the dissolution rates of minerals. Geochimica and Cosmochimica Acta, 52, 1969-1981.

Williamson, M.A., Rimstidt, J.D., 1994. The kinetics and electrochemical rate-determining step of aqueous pyrite oxidation. Geochimica and Cosmochimica Acta, 58, 5443-5454.

Wolery, T.J., 1992. EQ3NR, a computer program for geochemical aqueous speciation-solubility calculations: theoretical manual, User's guide, and related documentation (version 7.0), Berkeley, CA, Lawrence Livermore National Lab, 246 pp.

Zhang, S., Li, J., Wang, Y., Hu, G., 2004. Dissolution kinetics of galena in acid NaCl solutions at 25-75ºC. Applied Geochemistry, 19, 835-841.

Manuscript received February 2004;
revision accepted July 2004.